

Turbulence and Multiphase Modelling of Oil-in-Water Dispersions in Stirred Cells

C.P. Booth, J.L. Leggoe, Z.M. Aman, and V.W. Lim

School of Mechanical and Chemical Engineering,
The University of Western Australia, Crawley, Western Australia, 6009, Australia

Abstract

During the blowout of a subsea oil well, the fate and sequestration of the oil depends strongly on the size of the droplets. The distribution of the droplet sizes is determined by the turbulence of the flow field, the interaction between the phases present in the flow and the conditions at the well head. As full scale experiments are not tractable, benchtop and pilot-scale experimental investigations have been designed to measure oil droplet sizes under varying shear conditions. To better characterise the turbulence generated under these laboratory conditions, we have deployed a Finite Volume Method (FVM) to numerically simulate turbulence generated in a sapphire autoclave apparatus. To validate the turbulence models, a test condition was simulated for a single-phase baffled tank, where fluid motion was maintained by a Rushton turbine operating at Reynolds number of 7300. Results from a Wall Modelled Large Eddy Simulation (WMLES) were compared against the published experimental and Wall Resolving LES data. This method, along with a multiphase model, has been applied to simulate an autoclave system in which a four-blade vane-and-baffle mixing impeller was used to disperse oil in saltwater at high pressure. The speed of the impeller blade was varied to simulate Reynolds numbers ranging from 1073 to 5378, facilitating comparison between the model results and the experimental data.

Introduction

The explosion on the Deepwater Horizon oil rig and the associated well rupture released approximately 5.4 million barrels of oil and gas into the Gulf of Mexico over a period of 86 days [6]. The fate of the oil was strongly determined by the interaction of the jet with the flow field immediately surrounding the ruptured riser, where the plume was initially broken up into the distribution of droplet sizes. To manage the spill, 2.9 million litres of the dispersants Corexit 9527® and 9500A® were applied near the wellhead [8]. The dispersants acted to lower the interfacial tension between the water and oil, allowing the formation of a fine oil-in-water dispersion. There remains an open question as to whether the dispersants played a significant role in reducing the size of the droplets, or if the natural turbulence was sufficient to generate fine oil droplet sizes that may remain sequestered in the water column for an extended period [3-6]. As full-scale experiments are not tractable, experiments at the benchtop and pilot-scale have been performed to calibrate DSD functions that use a combination of the Reynolds, Weber and Viscosity numbers. Two broad categories of experiments can be identified; the jet geometry used by Brandvik et al. [5], and autoclave geometry used by Aman et al. [3]. There remains uncertainty as to the nature of the turbulence generated by the autoclave apparatus, and how it compares to the turbulence generated in a blowout [1]. The motivation of the present work is to simulate and quantify the relevant length scales and intensity of turbulence in the autoclave apparatus, to provide a benchmark for comparison with jet geometries.

Method

To directly simulate the experiments conducted by Aman et al. [3], the resolution of the simulation mesh must be comparable to the finest scales of motion given by the Kolmogorov Length (η),

$$\eta = \left(\frac{\nu^3}{\epsilon} \right)^{1/4} \quad (1)$$

where ν is the kinematic viscosity and ϵ the rate of dissipation of the turbulent energy. These definitions illustrate that the mesh size required to resolve these finest eddies scales with $Re^{9/4}$. The largest Reynolds number investigated by Aman et al. [3] would require a mesh on the order of 200 million elements. For comparative purposes, the smallest droplets observed by Aman et al. [3] had a diameter of 23 μm , and the simulated autoclave has a volume of 67000 mm^3 . If we consider that a droplet should be resolved by at least 10 elements in each direction, then a uniform mesh would require at least 1 trillion elements. As neither of these conditions could be met with the computational resources available, the current study has focussed on modelling the turbulent statistics at larger length scales, with the results used to estimate the smallest available droplet sizes.

One of the methods available to estimate the arithmetic mean droplet diameter is based on scaling laws based from the Weber and Reynolds dimensionless quantities. Based on oil-in-water dispersion data, Aman et al. [3] deployed a modified scaling relationship originally proposed by Boxall [4] for water-in-oil dispersions:

$$d_{50} = C_1 D We^{-3/5} \quad (2)$$

where d_{50} is the mean diameter of the droplet distribution, D is the length scale of the flow, We the Weber number, and C_1 a tuning constant which was determined to be 0.1 by Aman et al. [3].

Other correlation functions may be constructed using resolved flow parameters. For example, Zhou and Kresta [7] proposed an empirical correlation based on the rate of turbulent dissipation, and a mean circulation time approximated by ND^2 , where N is the rotational velocity:

$$d_{32} = 118.6(\epsilon_{\text{max}} ND^2)^{-2.70} \quad (3)$$

Computational Fluid Dynamics (CFD) is a unique tool capable of directly estimating the energy dissipation rate in varying mixing geometries, instead of relying on engineering approximations.

The autoclave used by Aman et al. [3] is idealised and shown in figure 1. The geometry used in the simulation had an outer cylinder diameter of 25.4 mm and the length was 150 mm; mixing was maintained through internal vane blades that had a diameter of 17.5 mm, a width of 1.75 mm and a total length of 120 mm. The vane was connected to a 15 mm shaft with a diameter of 4 mm, allowing a clearance of 15 mm at the base of the apparatus for measurements of fluid temperature (detailed by Aman et al. [3]) The baffles run the full length of the autoclave and are square prisms with sides lengths of 1.75 mm.

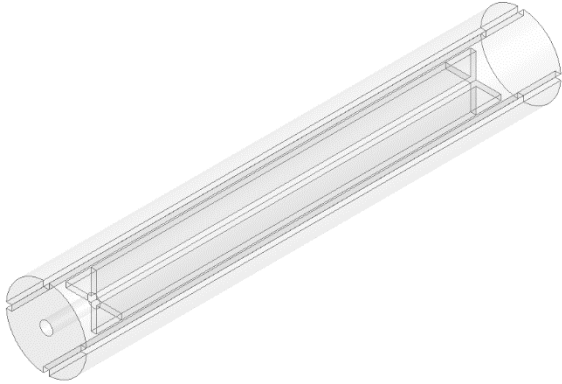


Figure 1: isometric view of autoclave geometry used to simulate the experiments of Aman et al. [3]

The characteristic length scale of the flow is the gap between the vane and the baffle, which was 22 mm in the present study. The length of the vane was 120 mm, delivering a ratio of 5.5 between the vane and gap. In initial simulations, it was assumed that this ratio is sufficient for the flow to be modelled as quasi-two dimensional (2D) for the central sections of the autoclave.

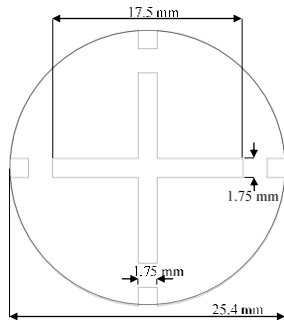


Figure 2: Geometry used for the 2D simulations showing key dimensions

The 2D geometry in figure 2 was used to characterise the flow in this experimental apparatus. The 2D simulation used the SST-k ω turbulence model with the momentum and turbulence discretised using a second order upwinding method. Pressure was discretised using a second order method and pressure-velocity coupling was handled by the SIMPLE method. The simulation was integrated in time using a second order implicit method with a constant time step. The fluid was set to the salt water used in [3], with a density of 1050 kg/m³ and a viscosity of 0.001 Pa.s. The simulations were run until the maximum turbulent dissipation had reached steady state value, which was then extracted every degree through at least five revolutions.

Figure 3 shows the mean droplet size predicted using equation 3 and the CFD results compared to the experimental results of Aman et al. [3]. We note that the agreement between the model and experiment is excellent at Reynolds numbers above 3000, but this accuracy decreases as the system approaches a laminar flow condition. Aman et al. [3] noted that, below the 500 RPM set

point, a significant volume fraction of oil was observed as a continuous liquid phase at the top of the autoclave; this lack of homogeneity may explain the disagreement observed in figure 3. Figure 4 compares the minimum Kolmogorov length scales to the smallest droplets observed by Aman et al. [3], which clearly demonstrates that the oil droplets were dispersed in the inertial subregime noted by Boxall [4]. For the range of Reynolds numbers considered here, the smallest Kolmogorov length provides a reasonable approximation of the smallest droplets that may be formed in the system; the formulation used in figure 3 is inherently limited, as a lack of explicit dependence on water-oil interfacial tension precludes the consideration of dispersant injection.

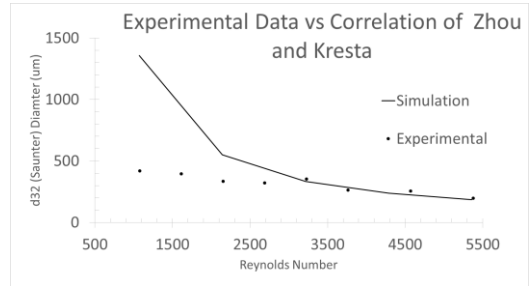


Figure 3: Mean droplet sizes from [3] as a function of Reynolds number compared against the correlation function of Zhou and Kresta [14] using the maximum dissipation rate determined by the 2D simulations.

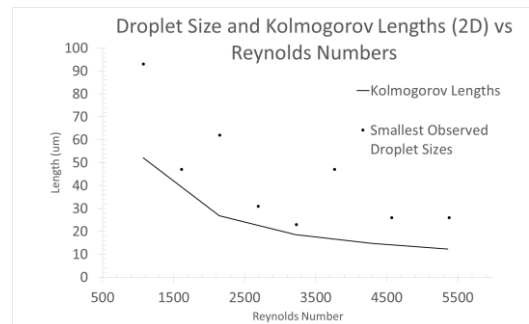


Figure 4: Smallest observed droplets by Aman et al [3] as a function of Reynolds number compared against the smallest Kolmogorov length determined using the simulation data.

Three-Dimensional (3D) Modelling

While the SST-k ω turbulence model performed well for the 2D simulations, strongly rotating 3D flows are better characterised by Large Eddy Simulation (LES) [7]. Unlike the RANS turbulence models, LES is derived using a spatial average and resolves the entire flow above the filter size, while the flow below the filter is modelled using a sub-grid scale model.

Deployment of LES is complicated by the fact that the largest eddies are small at the wall boundary layer. To accurately capture the near-wall effects, a considerable number of elements is required. To avoid this requirement, the boundary layer can be modelled using a RANS approach that doesn't have the same fine mesh requirements as the LES model. This work uses the Wall Modelled LES of Shur et al [10], where the inner part of the logarithmic layer was modelled using RANS and the rest of the boundary layer was resolved using LES. To test the capabilities of the WMLES formulation available in Fluent® v16.2, a simulation of a Rushton Turbine was performed and compared against experimental and simulation data collected by Hartmann et al [7]. The simulations performed by Hartmann et al [7] used a SST-k ω model and two LES models with different SGS models by Smagorinsky [11] (equation 4) and Voke [12] (equation 5).

$$\mu_t = \lambda_{mix} |S| \quad (4)$$

$$\mu_{t,V} = \mu_t - \beta\mu \left(1 - e^{-(\mu_t / \beta\mu)}\right) \quad (5)$$

where λ_{mix} is a length scale defined by

$$\lambda_{mix} = c_s \Delta \left(1 - e^{-(y^+ / A^+)}\right) \quad (6)$$

Where S is the strain-rate tensor, Δ is the cell size, c_s , β , and A^+ are constants, and y^+ is the non-dimensional wall distance. The Smagorinsky model typical uses a constant length $\lambda = c_s \Delta$, the additional term is from Van Driest [13] and acts to damp the viscosity close to the wall. The WMLES formulation uses a hybrid length scale to determine the eddy viscosity [2] that was modified from the original provided by Shur et al. [10]:

$$v_t = \min \left[(k d_w)^2, (c_s \Delta)^2 \right] \cdot S \cdot \left(1 - e^{-\left(\frac{y^+}{25}\right)^3} \right) \quad (7)$$

where d_w is the wall distance, k a constant.

Similar to Hartmann et al [7], we modelled the apparatus using two separate sections communicating through an interface. The outer annulus section containing the baffles was meshed using pure hexahedral elements, while the inner cylindrical section was modelled using a hybrid approach; the top and bottom sections were meshed using hexahedral elements and the central section around the blades was meshed using a tetrahedral/pyramidal. To simulate the motion of the turbine, the sliding mesh method was used. The simulation was run until the system reached a steady state; statistical data was then collected based on sampling the system 360 times per revolution for seven revolutions. Following Hartmann et al [7], the turbulent kinetic energy (TKE) was calculated through the spatial and temporal average velocity distributions:

$$TKE = \frac{1}{2} \left(\left\langle u_{i,\theta}^2 \right\rangle - \left\langle u_{i,\theta} \right\rangle^2 \right) \quad (8)$$

The data for the velocity and TKE profiles was collected from an axial line at $r/T = 0.183$, where T is the diameter of the apparatus, at an angle midway between two baffles.

Figures 5 to 7 illustrate the results of the present WMLES models, which agreed well with the numerical and experimental results of Hartmann et al [7]. While all four numerical results significantly overshoot the tangential velocity profile, the WMLES model performed the best with an average absolute deviation of 0.0742. The TKE profiles illustrate that, while the shape of the WMLES matches the experimental and other LES models, the magnitude is roughly half of what would be expected. Considering the excellent agreement between the radial profiles and the reasonable agreement with the tangential profiles, this difference in magnitude may be due to excessive element sizes that reduced the resolution in the axial direction.

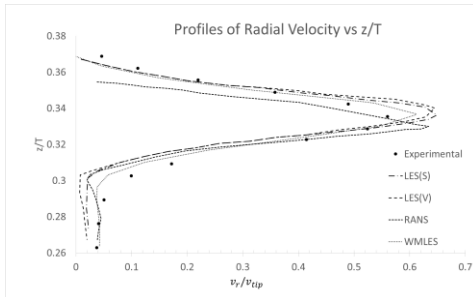


Figure 5: Averaged axial plots of the radial velocity for the simulations and experimental data for a line at $r/T = 0.183$

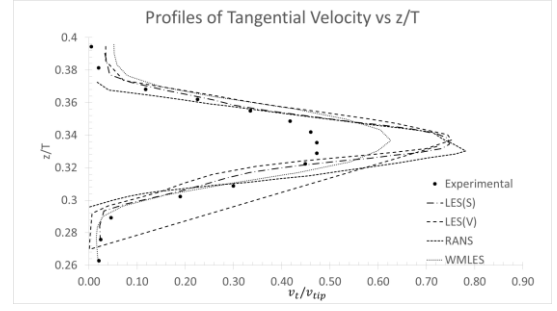


Figure 6: Averaged axial plots of the tangential velocity for the simulations and experimental data for a line at $r/T = 0.183$

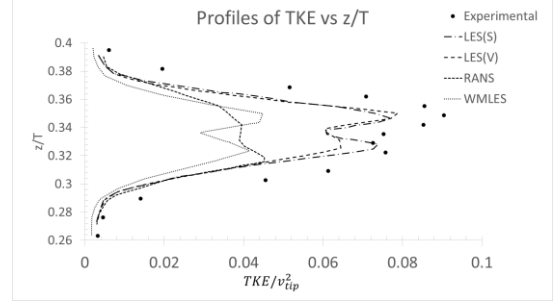


Figure 7: Averaged axial plots of the turbulent kinetic energy for the simulations and experimental data for a line at $r/T = 0.183$

Considering the severe resolution requirements for a 3D simulation discussed above and the results of the WMLES simulations above, the 3D simulations of the autoclave given in figure 1 were used to characterise the behaviour of the bulk motion at the highest and lowest set points observed in the experiments of Aman et al. [3]. Turbulence was modelled using WMLES for both autoclave models considered herein, the mesh used 1.2 million elements and is shown in figure 8. The oil phase was modelled based on the physical properties reported by Aman et al. [3], with a density of 700 kg/m^3 and a viscosity of 0.002 Pa.s . A coupled Volume of Fluid (VOF)-Level Set approach was used to model the multiphase system, with the continuum surface force defined by a surface tension of 20 mN/m . The model was initialised with the equivalent of 0.0688 g of water, where 0.001 g of oil was added in at the top of the simulation.

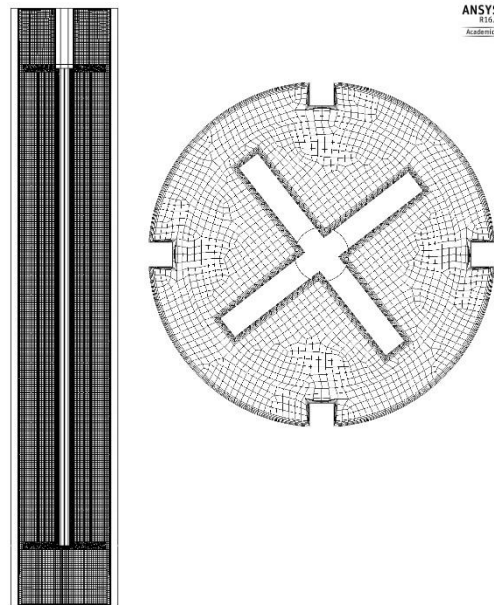


Figure 8: XY and ZY centre plane views of the mesh used in the 3D autoclave simulations

The simulations follow the same general behaviour as was observed by Aman et al. [3]. At 200 RPM, the oil remained as a continuous phase at the top of the autoclave with minimal interfacial disruption. While Aman et al. [3] did see droplets form in the 200 RPM case, the simulations did not have sufficient spatial resolution to capture this heterogeneous condition. Figures 10 and 11 illustrate isocontours of oil volume fraction at 0.5 and 0.1 collected for the autoclave at 1000RPM; these results illustrate that the oil was drawn down through the centre of vanes and then dispersed through the continuous phase. The models also highlight that potential usefulness of 2D models to expedite simulation cases, in the limit where the oil phase may be homogeneously dispersed.

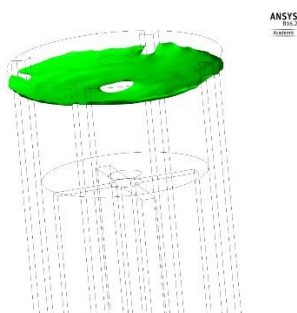


Figure 9: Isocontour of the volume fraction of 0.5 of oil at 200RPM



Figure 10: Isocontour of an oil volume fraction of 0.1 at 1000RPM

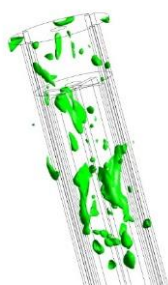


Figure 11: Isocontour of an oil volume fraction of 0.5 at 1000RPM

Conclusion

The results presented here illustrate that, for higher Reynolds numbers, 2D simulations and the formula determined by Zhou and Kresta [14] provide a good approximation for the mean size of the droplets, where the minimum Kolmogorov length scales provide a reasonable lower limit to the droplets. The 3D simulations of the autoclave show that, for low Reynolds numbers, the interface remains undisturbed and the requirement for quasi-2D conditions is not achieved. For higher Reynolds numbers, the oil phase is drawn towards the centre of the autoclave and homogeneously dispersed through the continuous phase. The WMLES model results for radial and tangential velocity profiles agreed well with established literature, suggesting that a hybrid length scale SGS viscosity model used

by the WMLES approach could potentially produce better profiles than either the standard Smagorinsky or the Voke models.

References

- [1] E. E. Adams, S. A. Socolofsky, and M. Boufadel, "Comment on "Evolution of the Macondo Well Blowout: Simulating the Effects of the Circulation and Synthetic Dispersants on the Subsea Oil Transport", " *Environmental Science & Technology*, vol. 47, pp. 11905-11905, 2013.
- [2] ANSYS Inc., "ANSYS® Academic Research, Release 16.2, ANSYS Fluent Theory Guide, ANSYS, Inc.," 2015.
- [3] Z. M. Aman, C. B. Paris, E. F. May, M. L. Johns, and D. Lindo-Atichati, "High-pressure visual experimental studies of oil-in-water dispersion droplet size," *Chemical Engineering Science*, vol. 127, pp. 392-400, 2015.
- [4] J. A. Boxall, C. A. Koh, E. D. Sloan, A. K. Sum, and D. T. Wu, "Droplet Size Scaling of Water-in-Oil Emulsions under Turbulent Flow," *Langmuir*, vol. 28, pp. 104-110, 2012.
- [5] P. J. Brandvik, Ø. Johansen, E. J. Davies, F. Leirvik, D. F. Krause, P. S. Daling, *et al.*, "Subsea Dispersant Injection - Summary of Operationally Relevant Findings From a Multi-Year Industry Initiative," 2016.
- [6] S. K. Griffiths, "Oil Release from Macondo Well MC252 Following the Deepwater Horizon Accident," *Environmental Science & Technology*, vol. 46, pp. 5616-5622, 2012.
- [7] H. Hartmann, J. J. Derksen, C. Montavon, J. Pearson, I. S. Hamill, and H. E. A. van den Akker, "Assessment of large eddy and RANS stirred tank simulations by means of LDA," *Chemical Engineering Science*, vol. 59, pp. 2419-2432, 2004.
- [8] E. B. Kujawinski, M. C. Kido Soule, D. L. Valentine, A. K. Boysen, K. Longnecker, and M. C. Redmond, "Fate of Dispersants Associated with the Deepwater Horizon Oil Spill," *Environmental Science & Technology*, vol. 45, pp. 1298-1306, 2011.
- [9] C. B. Paris, M. L. Hénaff, Z. M. Aman, A. Subramaniam, J. Helgers, D.-P. Wang, *et al.*, "Evolution of the Macondo Well Blowout: Simulating the Effects of the Circulation and Synthetic Dispersants on the Subsea Oil Transport," *Environmental Science & Technology*, vol. 46, pp. 13293-13302, 2012.
- [10] M. L. Shur, P. R. Spalart, M. K. Strelets, and A. K. Travin, "A hybrid RANS-LES approach with delayed-DES and wall-modelled LES capabilities," *International Journal of Heat and Fluid Flow*, vol. 29, pp. 1638-1649, 2008.
- [11] S. J. Smagorinsky "GENERAL CIRCULATION EXPERIMENTS WITH THE PRIMITIVE EQUATIONS," *Monthly Weather Review*, vol. 91, pp. 99-164, 1963.
- [12] P. R. Voke, "Subgrid-scale modelling at low mesh reynolds number," *Theoretical and Computational Fluid Dynamics*, vol. 8, pp. 131-143, 1996.
- [13] E. R. Van Driest, "On Turbulent Flow Near a Wall," *Journal of the Aeronautical Sciences*, vol. 23, pp. 1007-1011, 2016/08/24 1956.
- [14] G. Zhou and S. M. Kresta, "Correlation of mean drop size and minimum drop size with the turbulence energy dissipation and the flow in an agitated tank," *Chemical Engineering Science*, vol. 53, pp. 2063-2079, 1998.